Proximity of the Nucleotide Binding Domains of the P-glycoprotein Multidrug Transporter to the Membrane Surface: A Resonance Energy Transfer Study†

Ronghua Liu and Frances J. Sharom*

Guelph-Waterloo Centre for Graduate Work in Chemistry and Biochemistry, Department of Chemistry and Biochemistry, University of Guelph, Guelph, Ontario, Canada N1G 2W1

Received December 10, 1997; Revised Manuscript Received February 24, 1998

ABSTRACT: Very little structural information is available for P-glycoprotein (Pgp), which has been implicated in the multidrug resistance of human tumors because of its ability to act as an ATP-driven efflux pump for hydrophobic compounds. Highly purified Pgp has been labeled on two cysteine residues with the fluorescence probe NBD-Cl (7-chloro-4-nitro-2,1,3-benzoxadiazole). We show that NBD labels the same cysteine residues as MIANS [2-(4-maleimidoanilino)naphthalene-6-sulfonic acid]; they are located within the Walker A motif of the nucleotide binding domain, close to the site where ATP binds. NBD- and MIANS-labeled Pgps were reconstituted by detergent dilution into phospholipid vesicles containing increasing mole fractions of rhodamine- or NBD-labeled phosphatidylethanolamine (PE), respectively. The fluorescence of the NBD-Pgp and MIANS-Pgp donors was quenched in a concentration-dependent manner by the rhodamine-PE and NBD-PE acceptors. Using two different methods to analyze Förster resonance energy transfer, the distance of the Pgp-bound probes from the lipid−water interfacial region of the bilayer was estimated to be 31−35 Å. This distance is compatible with the low-resolution structure of Pgp determined by electron microscopy, and indicates that the nucleotide binding domains lie close to the membrane surface. The experimental data fitted very well to theoretical quench curves for a single protein-bound fluor, suggesting that the two nucleotide binding domains are located equidistant from the bilayer. Following the addition of ATP to MIANS-Pgp, the NBD-PE quench curve no longer conformed to the models. These results imply that Pgp interacts differently with PE when it is in the ATP-bound form.

Members of the ABC[1] (ATP binding cassette) or traffic ATPase superfamily of proteins (*1, 2*) are involved in translocation of various compounds across cellular membranes. The most important hallmark of the ABC proteins is the presence of one or more NB (nucleotide binding) domains. These domains, which are the most highly conserved elements of the protein family, are involved in the coupling of ATP hydrolysis to transport of substrates across the membrane. Important eukaryotic ABC proteins include the cystic fibrosis transmembrane conductance regulator (CFTR), the yeast *a*-factor mating peptide exporter STE6, the TAP1/2 peptide transporters of the endoplasmic reticulum, and the P-glycoprotein (Pgp) family, which comprises the class I and II gene products (multidrug transporters) and the class III gene product (a phosphatidylcholine flippase). The Pgp multidrug transporter functions as an ATP-driven efflux pump for a structurally diverse group of hydrophobic natural products, drugs, and peptides, and is believed to play an important role in the resistance of several human tumors to chemotherapeutic drugs. For more details of the molecular biology, structure, and function of Pgp, the reader is referred to several recent comprehensive reviews (*3*−*6*).

There is currently very little structural information available for Pgp. Hydropathy analysis of the amino acid sequence predicts the existence of 12 membrane-spanning segments, and 2 putative NB domains on the cytosolic side of the membrane. Several features of this model have been confirmed by epitope insertion (*7*), and engineering of cysteine residues in strategic locations followed by determination of their accessibility to membrane-permeant and -impermeant labeling reagents (*8*). The overall contributions of α-helix, *β*-sheet, turns, and random coil to the secondary structure of Pgp have been estimated by Fourier transform infrared spectroscopy (*9*). Rosenberg et al. (*10*) have recently determined a low-resolution structure of Pgp (to 2.5 nm) using electron microscopy and image reconstruction. The Pgp molecule appeared to be a toroidal structure of 6-fold symmetry, with two 3 nm lobes at the cytoplasmic face of the membrane which were proposed to correspond to the NB domains.

†This work was supported by a grant to F.J.S. from the National Cancer Institute of Canada, with funds provided by the Canadian Cancer Society.

* To whom correspondence should be addressed (telephone, 519-824-4120, ext 2247; FAX, 519-766-1499; e-mail, sharom@chembio.uoguelph.ca).

[1] Abbreviations: ABC, ATP binding cassette; CFTR, cystic fibrosis transmembrane conductance regulator; CHAPS, 3-[(3-cholamidopropyl)dimethylammonio]-1-propanesulfonate; DTE, dithioerythritol; FRET, Förster resonance energy transfer; GuHCl, guanidine hydrochloride; NAc-Cys, *N*-acetyl-L-cysteine; NAc-Lys-ME, *N*-acetyl-L-lysine methyl ester; MDR, multidrug resistance; MIANS, 2-(4-maleimidoanilino)-naphthalene-6-sulfonic acid; NB, nucleotide binding; NBD-Cl, 7-chloro-4-nitro-2,1,3-benzoxadiazole; PC, phosphatidylcholine; PE, phosphatidylethanolamine; Pgp, P-glycoprotein; QELS, quasi-elastic light scattering; LRhoB, Lissamine rhodamine B.

S0006-2960(97)03031-6 CCC: $15.00
Published on Web 04/16/1998

During the past few years, methods have been developed to purify relatively large amounts of full-length Pgp, and reconstitution of the ATPase activity and drug transport functions of the protein in lipid bilayers has been achieved (for a review, see *6*). These advances have made it possible to use powerful spectroscopic methods, such as fluorescence, to provide insights into Pgp structure and dynamics. Recent studies in our laboratory have shown that a long-range conformational change takes place following binding of drugs (*11*). We have also demonstrated the existence of conformational communication between the site(s) of drug binding and the ATPase catalytic sites (*11*). More recently, the molecular characteristics of the NB domains of Pgp were examined using collisional quenching, and binding of fluorescent ATP derivatives (*12*).

The technique of Förster resonance energy transfer (FRET) can be used as a "spectroscopic ruler" to measure inter- and intramolecular distances in proteins, and the distance between a defined site in a protein and the membrane. FRET has proved very useful in delineating structural details of several membrane proteins and transporters. For the Ca^{2+}-ATPase, it allowed estimation of the distance of the ATP and Ca^{2+} binding sites from the membrane surface (*13*, *14*), the location of an active site lysine residue relative to several probes within the lipid bilayer (*15*), and the distances between several cysteine residues and the active site lysine (*16*). FRET also showed that the epidermal growth factor binding site within its receptor was distant from the membrane (*17*), whereas the α, β, and γ subunits of a heterotrimeric G-protein were located close to the bilayer surface (*18*). Changes in location can also be detected using FRET; the distance from the phospholipid surface of the catalytic site of activated protein C was found to be altered by interaction with protein S (*19*).

The present study describes the first application of FRET in probing the topography of the Pgp molecule. Using a purified reconstituted system, we have estimated the distance from the host bilayer of a defined location within the ATPase catalytic site of Pgp. Results indicate that the NB domains are equivalently positioned close to the membrane surface. Evidence is also presented which suggests that binding of ATP to the catalytic sites changes the interaction of Pgp with membrane lipids.

MATERIALS AND METHODS

Materials. Egg PC and egg PE were obtained from Avanti Polar Lipids Inc. (Alabaster, AL). The fluorescently labeled lipids (7-nitrobenz-2-oxa-1,3-diazol-4-yl)-1,2-dihexadecanoyl-*sn*-glycero-3-phosphoethanolamine (NBD-PE; triethylammonium salt) and Lissamine rhodamine β-1,2-dihexadecanoyl-*sn*-glycero-3-phosphoethanolamine (LRhoB-PE; triethylammonium salt) and the fluorescence probe 2-(4-maleimidoanilino)naphthalene-6-sulfonic acid (MIANS) were obtained from Molecular Probes (Eugene, OR). Dithioerythritol (DTE), *N*-acetyl-L-cysteine (NAc-Cys), *N*-acetyl-L-lysine methyl ester (NAc-Lys-ME), Na_2-ATP, 3-[(3-cholamidopropyl)dimethylammonio]-1-propanesulfonate (CHAPS), 7-chloro-4-nitro-2,1,3-benzoxadiazole (NBD-Cl), and guanidine hydrochloride (GuHCl) were supplied by Sigma Chemical Co. (St. Louis, MO).

Characterization of NBD-Cl, S-NBD-NAc-Cys, and N-NBD-NAc-Lys-ME. A 100 mM stock solution of NBD-Cl was prepared in methanol, and a 100 μM solution of NBD-Cl was freshly prepared by adding the stock solution to 50 mM Tris-HCl buffer (pH 7.5) immediately before spectral analysis, since NBD-Cl undergoes hydrolysis in aqueous buffer. S-NBD-NAc-Cys (NAc-Cys labeled with NBD on the thiol group) was prepared by incubating 100 μM NBD-Cl with 1 mM NAc-Cys in 50 mM Tris-HCl buffer (pH 7.5). Absorption, fluorescence excitation, and fluorescence emission spectra were run within 2 h, since S-NBD-NAc-Cys is not very stable in aqueous solution. N-NBD-NAc-Lys-ME (NAc-Lys-ME labeled with NBD on the γ-NH_2 group) was prepared by incubating 100 μM NBD-Cl with 1 mM NAc-Lys-ME in Tris-HCl buffer (pH 9.5) at 22 °C for 24 h. The pH was adjusted to 7.5 before running absorption, fluorescence excitation, and fluorescence emission spectra. Samples containing 100 μM NBD were used directly for absorbance measurements, and diluted with 50 mM Tris-HCl buffer (pH 7.5) to 20 μM for fluorescence measurements.

Absorption Spectra and Fluorescence Excitation and Emission Spectra. Absorption spectra were recorded using a computer-interfaced Perkin-Elmer Lambda 6 UV/visible spectrophotometer (Perkin-Elmer, Norwalk, CT) with both sample and reference cells at 22 °C. Fluorescence spectra were recorded on a PTI Alphascan-2 spectrofluorimeter (Photon Technology International, London, Ontario, Canada) with the cell holder thermostated at 22 °C. All spectra were measured with a 4 nm excitation and emission band-pass. Emission spectra of MIANS-Pgp and NBD-Pgp were corrected using a built-in automatic correction system. Each sample was scanned 3 times, and the final fluorescence spectrum represents the average spectrum of three or more samples.

Fluorescent Labeling of Pgp. Purified Pgp was labeled with MIANS as described previously (*11*). To fully label Pgp with NBD, CH^RB30 plasma membrane was suspended at a concentration of 4 mg/mL in 50 mM Tris-HCl/0.15 M NaCl/5 mM $MgCl_2$/0.02% Na_3 (pH 7.5), and 100 mM NBD-Cl stock solution was added to give a final concentration of 1 mM. The membrane sample was incubated at 22 °C for 2 h, and then washed 3 times with 50 mM Tris-HCl buffer by centrifugation at 100000*g* for 30 min. NBD-Pgp was purified from NBD-labeled plasma membrane as described below.

Preparation of Reconstituted Vesicles Containing Pgp. Highly purified Pgp (>95% pure) was isolated from the plasma membrane of MDR CH^RB30 Chinese hamster ovary cells essentially as reported previously (*11*, *12*), with the following modifications. The partially purified S_2 fraction was prepared using 8 mM CHAPS and 0.25 M sucrose in a buffer consisting of 50 mM Tris-HCl/0.15 M NaCl/5 mM $MgCl_2$/0.02% Na_3 (pH 7.5), and Pgp was further purified by concanavalin A−Sepharose chromatography using 2 mM CHAPS and 0.25 M sucrose in the same buffer. Pgp from NBD-labeled CH^RB30 plasma membrane was isolated using the same method. Purified Pgp was quantitated using the method of Peterson (*20*).

MIANS- or NBD-labeled Pgp was reconstituted into phospholipid vesicles by a detergent dilution method. Stock solutions of egg PC, egg PE, NBD-PE, and LRhoB-PE were prepared in CH_3Cl−MeOH and stored at −20 °C. Egg PC (0.075 μmol) and a mixture of egg PE and the appropriate amount of either NBD-PE or LRhoB-PE (total PE 0.075

μmol) were dispensed into a series of microcentrifuge tubes, mixed, dried under a gentle stream of nitrogen, and then pumped under vacuum for 1 h. Following the addition of 10 μL of 25 mM CHAPS/0.25 M sucrose in 50 mM Tris-HCl buffer (pH 7.5), the contents of each tube were vortexed, and then sonicated for 5 min in a Sonogen sonicator (Branson Instruments, Inc., Stamford, CT). MIANS-Pgp or NBD-Pgp (18 μg in 30 μL of 2 mM CHAPS/0.25 M sucrose/Tris-HCl buffer) was then added to each, and the tubes were incubated for 30 min on ice. Samples were then diluted with 560 μL of 0.25 M sucrose/Tris-HCl buffer, resuspended using a fine-gauge needle, and kept on ice for 4−12 h. The final lipid concentration was 0.25 mM, and the protein concentration was 30 μg/mL, with a lipid:protein mole ratio of 1420:1. Control vesicles containing the same amount of unlabeled Pgp were prepared in the same way. The size distribution of the reconstituted vesicles was determined using quasi-elastic light scattering (QELS) as described previously (*21*).

Measurement of Pgp ATPase Activity. The Mg^{2+}-dependent ATPase activity of Pgp was measured by the method of Doige et al. (*22*) in the presence of 1 mM ATP and 5 mM Mg^{2+}. To quantitate inhibition of Pgp ATPase activity, various concentrations of NBD-Cl were preincubated with purified Pgp in 2 mM CHAPS/0.25 M sucrose/Tris-HCl buffer (pH 7.5) for 20 min at 22 °C. Unreacted NBD-Cl was deactivated with 2 mM DTE before initiation of the ATPase assay by addition of ATP. Heat-inactivated Pgp samples treated with various concentrations of NBD-Cl were used as controls.

Determination of the Stoichiometry of NBD Labeling. To determine the stoichiometry of labeling of Pgp with NBD, purified NBD-Pgp samples were dialyzed against 3 × 1 L of 50 mM ammonium bicarbonate at 4 °C in the dark. Following lyophilization, the samples were redissolved at a protein concentration of 0.5−0.9 mg/mL in 6 M GuHCl/50 mM Tris-HCl (pH 7.5). Covalently bound NBD was quantitated by absorbance measurement at 430 nm using an extinction coefficient for NBD-labeled cysteine in proteins of 13 000 M^{-1} cm^{-1} (*23*). Blanks containing the same concentration of unlabeled Pgp were treated the same way as the NBD-labeled samples and used to correct the absorbance data. Labeling stoichiometry was assessed using three independent batches of NBD-labeled Pgp. The molar mass of Pgp polypeptide used for stoichiometry calculations was 140 kDa.

Resonance Energy Transfer Measurements. Fluorescence intensities were measured using a Spex Model DM 3000 spectrofluorimeter (Spex Industries Inc., South Brunswick, NJ). The excitation wavelengths for MIANS-Pgp and NBD-Pgp were 322 and 465 nm, respectively, while emission was monitored at 420 and 523 nm, respectively, with 4 nm slits. Measured fluorescence intensities were corrected for light scattering using controls containing unlabeled Pgp. The inner filter effect was corrected at both the excitation and emission wavelengths as described previously (*11*, *24*, *25*) using the equation:

$$F_{icor} = (F_i - B)10^{0.5b(A_{\lambda ex}+A_{\lambda em})} \quad (1)$$

where F_{icor} is the corrected value of the fluorescence intensity, F_i is the experimentally measured fluorescence intensity, B is the background fluorescence intensity (caused mainly by lipid vesicle scattering), b is the path length of the optical cell in centimeters, and $A_{\lambda ex}$ and $A_{\lambda em}$ are the absorbances of the sample at the excitation and emission wavelengths, respectively.

Determination of Parameters for FRET Analysis. The efficiency of resonance energy transfer (E) between the donor and acceptor can be written as

$$E = 1 - F/F_o \quad (2)$$

where F and F_o are the fluorescence intensities of the donor in the presence and absence of the acceptor, respectively. The efficiency of FRET is related to the inverse sixth power of the distance (R) between the donor and acceptor in an isolated donor−acceptor system

$$R = R_o(E^{-1} - 1)^{1/6} \quad (3)$$

where R_o is the distance at which the efficiency of energy transfer is 50%. R_o can be calculated from

$$R_o = (9.8 \times 10^3)(J\kappa^2 Q_D n^{-4})^{1/6}\ (\text{Å}) \quad (4)$$

where J is the spectral overlap integral between donor and acceptor in units of $cm^3\ M^{-1}$ (see Table 2). The orientation factor κ^2 was taken as 2/3. Small differences between the true and assumed values of κ^2 produce only small errors in calculated donor−acceptor distances (*26*). In addition, there is a particularly small error for energy transfer from a protein-bound donor to a phospholipid acceptor because of the random orientation of acceptor fluorophores in the lipid bilayer (*27*). Q_D is the fluorescence quantum yield of the donor, and n is the refractive index of the medium between the chromophores, which was taken as 1.33, that of a dilute aqueous solution (*28*).

The spectral overlap integral (J) was determined using the integral equation:

$$J = \frac{\int F_D(\lambda)\epsilon_A(\lambda)\lambda^4\,\delta\lambda}{\int F_D(\lambda)\,\delta\lambda} \quad (5)$$

where F_D is the fluorescence intensity per unit wavelength interval in the presence of donor only, ϵ_A is the molar extinction coefficient of the acceptor, and λ is the wavelength in centimeters. The fluorescence emission spectra of MIANS-Pgp and NBD-Pgp were recorded using excitation at 322 and 465 nm, respectively, and the absorption spectra of NBD-PE and LRhoB-PE were measured. J was calculated from the spectral data using a computer program designed solely for that purpose by Dr. Uwe Oehler (Department of Chemistry and Biochemistry, University of Guelph).

The quantum yields, Q_D, of MIANS-Pgp and NBD-Pgp in reconstituted vesicles were determined relative to standards, using polarizers oriented at the magic angle (54.7°) in both the excitation and emission beams. The fluorescence emission spectra of MIANS-Pgp and a standard solution of quinine sulfate in 0.1 N H_2SO_4 were measured using an excitation wavelength of 322 nm. Both the sample and standard had the same absorbance value of 0.095 at 322 nm. The quantum yield of MIANS-Pgp was calculated using the equation:

$$Q_{\mathrm{MIANS-Pgp}} = \frac{F_{\mathrm{MIANS-Pgp}}}{F_{\mathrm{quinine}}} \times Q_{\mathrm{quinine}} \quad (6)$$

where Q_{quinine}, the quantum yield of quinine, is known to be 0.51 in 0.1 N H_2SO_4 (*29*), and $F_{\mathrm{MIANS-Pgp}}$ and F_{quinine} are the integrals of the fluorescence of MIANS-Pgp and quinine sulfate in the wavelength range 350−600 nm, respectively. Similarly, the quantum yield of NBD-Pgp was determined relative to a standard solution of fluorescein in 0.1 N NaOH using 0.91 as the value of $Q_{\mathrm{fluorescein}}$ (*29*), over an integral wavelength range of 475−700 nm. Measurements were made on solutions of NBD-Pgp and fluorescein having the same absorbance of 0.095 at the excitation wavelength of 465 nm. For both MIANS-Pgp and NBD-Pgp, scattering was corrected with reconstituted vesicles containing unlabeled Pgp at the same protein concentration.

Analysis of the Distance between Donor and Acceptor. The data for energy transfer between the MIANS-Pgp/NBD-PE pair and the NBD-Pgp/LRhoB-PE pair were analyzed by two approaches. The first approach is that of Koppel et al. (*30*), in which the donors and acceptors are assumed to lie on spherical shells of radius $R \pm h$ and R, respectively, where each is confined to one or the other monolayers of the bilayer vesicle. Thus, h is the distance of closest approach of the donor to the acceptor. In general, h can be positive (if the donor is above the plane of the lipid bilayer) or negative (if the donor is below the plane of the lipid bilayer or buried in it). The acceptors are considered to be randomly distributed on the surface of each vesicle. Koppel et al. showed that energy transfer can be represented by the equation:

$$\sigma = \frac{0.62}{\pi {R_o}^2} \times \frac{R-h}{R} \times \left(\frac{E}{1-E}\right)^{0.91} \times e^{(-0.34r+1.63r^2)} \quad (7)$$

where σ is the acceptor surface density (number per Å^2), R is the average radius of the vesicles, and r is defined as $r = h/R_o$. Using eq 2, the above can be rearranged as

$$\frac{F_o}{F_o - F} = 1 + \sigma^{-1.1}\left[\frac{0.62}{\pi {R_o}^2} \times \frac{R-h}{R} \times e^{(-0.34r+1.63r^2)}\right]^{1.1} \quad (8)$$

If the average surface area of a phospholipid molecule is assumed to be 80 Å^2, then σ can be calculated as

$$\sigma = N \times \frac{1}{80}\ (\text{Å}^{-2}) \quad (9)$$

where N is the mole ratio of acceptors to total phospholipids.

The second approach employed is that of Dewey and Hammes (*31*), which assumes that the donors are uniformly distributed on one plane and the acceptors on another plane, the two planes being parallel and separated by a distance h. Dewey and Hammes showed that the extent of quenching of the donor fluorescence was given approximately by

$$\frac{F}{F_o} = \frac{A_2 + A_3}{2} \quad (10)$$

where

$$A_2 = \left[1 + 0.4\left(\frac{R_o}{h}\right)^6\right]\left[1 + 0.4\left(\frac{R_o}{h}\right)^6 + \left(\frac{\pi\sigma {R_o}^2}{2}\right)\left(\frac{R_o}{h}\right)^4\right]^{-1} \quad (11)$$

and

$$A_3 = \left[1 + \left(\frac{\pi\sigma {R_o}^2}{2}\right)\left(\frac{R_o}{h}\right)^4 + 0.625\left(\frac{R_o}{h}\right)^6\right] \times \left\{\left[1 + \left(\frac{\pi\sigma {R_o}^2}{2}\right)\left(\frac{R_o}{h}\right)^4\right]^2 + \left[1 + \left(\frac{\pi\sigma {R_o}^2}{2}\right)\left(\frac{R_o}{h}\right)^4\right]0.625\left(\frac{R_o}{h}\right)^6 - \left(\frac{\pi\sigma {R_o}^2}{5}\right)\left(\frac{R_o}{h}\right)^{10}\right\}^{-1} \quad (12)$$

Curve fitting was carried out using SigmaPlot for Windows (SPSS Inc., Chicago, IL), and the distances between the donor and acceptor were extracted.

The two approaches used to analyze the FRET data do not take account of the fact that the membrane-bound domain of Pgp will effectively exclude lipid acceptors from a certain volume of the bilayer. Accounting for "dead space" or excluded volume effects is difficult in this case, since very little is known about the size and geometry of the membrane-bound and NB domains of Pgp, or their spatial orientation relative to each other. A detailed treatment of such effects has been described by Wolber and Hudson (*32*) for a simple system where the donors and acceptors are located in a plane, and the donors exclude the acceptors from a spherical shell. The effect of excluded volume is to reduce the observed quenching of the donor by the acceptor, relative to the quenching that would be expected if no excluded volume effects were present (*32*); i.e., if excluded volume effects are in existence, a higher acceptor concentration in the membrane is needed to achieve the same level of quenching. In the present study, the "true" value of h, accounting for excluded volume effects, would be smaller than h calculated from the models of Koppel and co-workers, and Dewey and Hammes. Therefore, the calculated values of h shown in Table 3 represent an upper limit for the distance of closest approach of the donor to the acceptor.

RESULTS

NBD Labeling of Pgp. NBD-Cl has been widely employed as an inhibitor of ATP-driven membrane transporters. NBD is a useful agent for covalent modification of proteins, since it is able to selectively label (depending on the pH of the reaction) cysteine, lysine, and tyrosine residues, giving characteristic UV−visible absorption spectra that can be used for their identification. The NBD group also becomes highly fluorescent following reaction with cysteine and lysine residues. As shown in Figure 1, the ATPase activity of highly purified Pgp is progressively abolished by reaction for 20 min at 22 °C with increasing concentrations of NBD-Cl, with complete loss of Pgp ATPase achieved following treatment with 1 mM NBD-Cl. The presence of 2 mM ATP largely prevented NBD-Cl inactivation of Pgp, although protection was not complete (Figure 1).

Attempts to label highly purified Pgp directly with NBD-Cl were unsatisfactory, since NBD-Cl reacted rapidly with

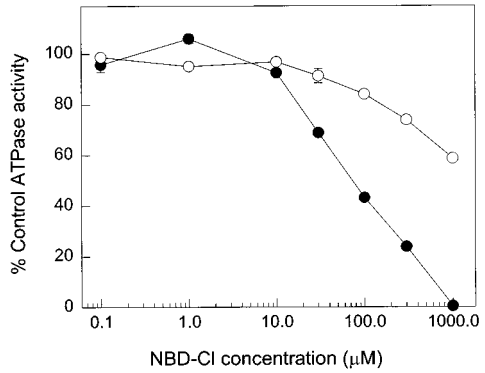

FIGURE 1: Inactivation of Pgp ATPase activity by the covalent modification reagent NBD-Cl. Purified Pgp (50 μg/mL in 2 mM CHAPS/0.25 M sucrose/Tris-HCl buffer, pH 7.5) was treated with increasing concentrations of NBD-Cl for 20 min at 22 °C. Pgp was treated with NBD-Cl in the absence (●) or presence (○) of 2 mM ATP. After rapid deactivation of unreacted NBD-Cl with 2 mM DTE, the ATPase activity was determined. Percent control ATPase activity was calculated relative to heat-inactivated Pgp samples and represents the mean ± SEM for triplicate determinations.

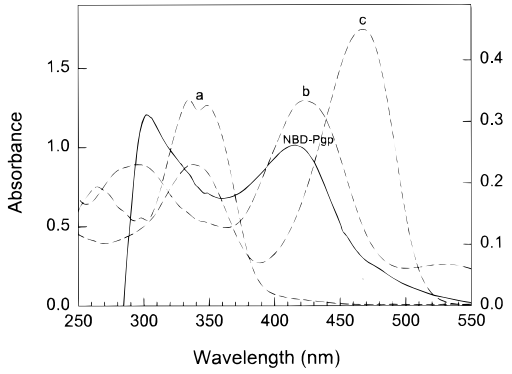

FIGURE 2: UV−visible absorption spectra of (a) NBD-Cl, (b) S-NBD-NAc-Cys, (c) N-NBD-NAc-Lys-ME (dashed lines; left absorbance scale) and 1.5 mg/mL NBD-Pgp (solid line; right absorbance scale) in 6 M GuHCl. Concentrations of NBD-Cl, S-NBD-NAc-Cys, and N-NBD-NAc-Lys-ME used were 100 μM.

the detergent CHAPS, whose presence is required to maintain Pgp solubility and activity. To achieve covalent modification of Pgp with NBD-Cl, an alternative approach was used where CH^RB30 plasma membrane was reacted with NBD-Cl, followed by purification of NBD-labeled Pgp from the plasma membrane. Complete labeling of Pgp was achieved by treatment of plasma membrane with 1 mM NBD-Cl for 2 h at 22 °C. Following complete inactivation of Pgp ATPase activity by NBD-Cl, the bound chromophore was quantitated by UV−visible absorption spectroscopy. Absorbance measurements of NBD-modified Pgp indicated the presence of 2.21 ± 0.02 (n = 3) mol of NBD/mol of Pgp. These results suggest that two NBD labels were covalently incorporated into each molecule of Pgp.

Spectroscopic analysis was used to identify the amino acid side chains in Pgp that had been labeled with NBD. Figure 2 shows the absorption spectra of NBD-Pgp compared to those of NBD-Cl, lysine NBD-labeled on the γ-amino group (N-NBD-NAc-Lys-ME), and cysteine NBD-labeled on the SH group (S-NBD-NAc-Cys). The absorption spectrum of NBD-Pgp in 6 M GuHCl closely resembled that of S-NBD-NAc-Cys, with the λ_{max} shifted slightly downward from 423 to 420 nm (see Table 1), which indicates that cysteine residues are the most likely targets of NBD labeling. Fluorescence spectroscopic characterization of the various NBD derivatives showed that the excitation maximum, emission maximum, and fluorescence intensity of S-NBD-NAc-Cys were very sensitive to the solvent. The λ_{ex} for S-NBD-NAc-Cys increased from 425 nm in aqueous buffer to 450−465 nm in nonpolar solvents (Table 1). The λ_{em} also increased from 523 to 530−534 nm in the less polar alcohol solvents, but λ_{em} declined to 522 nm in the most nonpolar solvent, 1,4-dioxane. Furthermore, S-NBD-NAc-Cys exhibited a relatively low intensity of fluorescence in aqueous buffer which increased 8−12-fold in nonpolar solvents, including 1,4-dioxane (Table 1). The fluorescence emission spectra of N-NBD-NAc-Lys-ME, S-NBD-NAc-Cys, and NBD-Pgp in both detergent solution and GuHCl are shown in Figure 3. The values of λ_{max} for excitation and emission and the relative fluorescence intensity for NBD-Pgp (Table 1) suggested that the probe is bound to cysteine, and is located in a relatively nonpolar local environment.

The NBD moiety becomes highly fluorescent following covalent reaction with proteins, allowing the labeling process to be readily followed in real time. To further investigate the sites of labeling within Pgp, NBD was added to either native Pgp or Pgp that had been previously labeled with MIANS. As shown in Figure 4A, NBD-Cl reacted rapidly with native Pgp, as indicated by an increase in fluorescence emission at 523 nm on excitation at 465 nm. In contrast, NBD failed to react with MIANS-labeled Pgp, which showed only a small change in fluorescence with time, which was essentially equivalent to that displayed by the buffer alone.

Table 1: Spectral Characteristics of NBD-Cl and NBD-Labeled Derivatives

			fluorescence		
compound	solvent	absorbance λ_{max} (nm)	excitation λ_{ex} (nm)	emission λ_{em} (nm)	relative intensity[a]
NBD-Cl	H_2O, pH 7.5	340	—[b]	—[b]	—[b]
S-NBD-NAc-Cys	H_2O, pH 7.5	423	425	523	1.0
	methanol	nd[c]	465	534	7.6
	1-butanol	nd	465	530	8.6
	1-octanol	nd	465	530	10.5
	1,4-dioxane	nd	450	522	12.4
NBD-Pgp	6 M GuHCl	420	465	536	11.9
	2 mM CHAPS	420	465	523	12.4
	lipid bilayers	nd	465	523	12.4
N-NBD-NAc-Lys-ME	H_2O, pH 7.5	465	465	550	10.3

[a] Fluorescence intensity at λ_{em} is expressed relative to that of S-NBD-NAc-Cys in aqueous buffer. [b] NBD-Cl is not fluorescent. [c] nd, not determined.

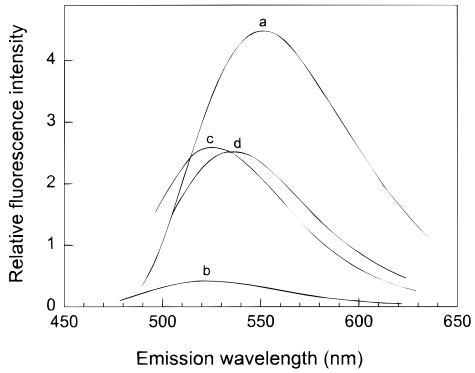

FIGURE 3: Fluorescence emission spectra upon excitation at 465 nm for (a) 20 μM N-NBD-NAc-Lys-ME, (b) 20 μM S-NBD-NAc-Cys, and 0.25 mg/mL NBD-Pgp in (c) 2 mM CHAPS and (d) 6 M GuHCl. Emission bandwidth was 4 nm.

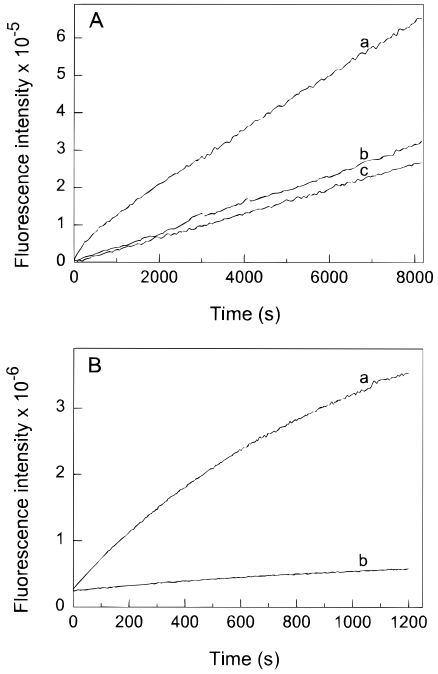

FIGURE 4: Reaction of Pgp with the fluorescence probes NBD-Cl and MIANS. Labeling with 100 μM NBD-Cl (A) was carried out at 22 °C with either (a) native Pgp (50 μg/mL in 2 mM CHAPS/0.25 M sucrose/Tris-HCl buffer, pH 7.5) or (b) MIANS-labeled Pgp (50 μg/mL in the same buffer). A control reaction, c, was carried out with NBD-Cl in the absence of Pgp, to assess its hydrolysis in the aqueous buffer. Labeling with 10 μM MIANS (B) was carried out at 22 °C with either (a) native Pgp (50 μg/mL in 2 mM CHAPS/0.25 M sucrose/Tris-HCl buffer, pH 7.5) or (b) NBD-labeled Pgp (50 μg/mL in the same buffer). For reactions using MIANS, excitation was at 322 nm and emission was monitored at 420 nm, while for reactions using NBD-Cl excitation and emission were at 465 and 523 nm, respectively, using emission bandwidths of 4 nm.

These results suggest that NBD reacts with the same two cysteine residues as MIANS. This proposal was further supported by experiments in which either native Pgp or Pgp previously labeled with NBD was reacted with MIANS. A large increase in fluorescence intensity at 420 nm with time was evident as MIANS covalently labeled Pgp, whereas NBD-labeled Pgp showed essentially no reaction (Figure 4B). We conclude that NBD-Cl covalently modifies Pgp at the same two cysteine residues that are labeled by MIANS, Cys 428 and 1071 (GCGKS) within the Walker A motifs of the NB domains.

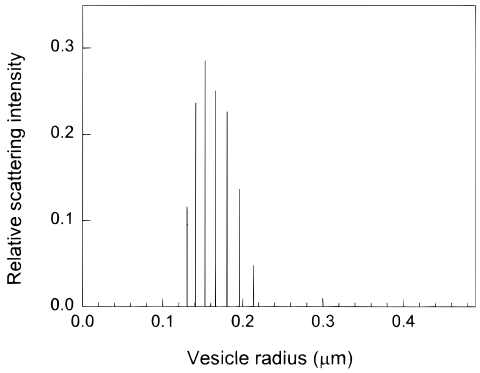

FIGURE 5: QELS measurement of the size distribution profile of reconstituted vesicles containing Pgp, prepared from CHAPS solution by detergent dilution. The vesicles were made up of 1:1 mol/mol egg PC/egg PE, and their lipid:protein ratio was ~6.3:1 w/w or 1420:1 mol/mol.

Reconstitution of MIANS- and NBD-Labeled Pgp with Fluorescent PE Derivatives. FRET requires fluorescently labeled donor and acceptor molecules. The two catalytic sites of the NB domains of Pgp were fluorescently labeled by covalent reaction with either MIANS or NBD-Cl, and acted as the donors. Labeled Pgp was then reconstituted into lipid bilayers of egg PC/egg PE by rapid detergent dilution. The membrane was fluorescently labeled by incorporation into the bilayer of PE derivatives containing either NBD or LRhoB in the polar headgroup. Labeled PE derivatives were chosen as the FRET acceptors since this species is present in the lipid annulus surrounding purified Pgp, and PE also activates the ATPase activity of Pgp (*33*, *34*). QELS analysis of the resulting reconstituted vesicles showed that they comprised a relatively homogeneous single population of large vesicles, with a narrow size distribution and a mean diameter of 0.31 μm (Figure 5).

Resonance Energy Transfer. To assess the relative distance of the ATPase catalytic sites of Pgp from the bilayer surface, energy transfer must take place between the NBD or MIANS donors at the active site of Pgp, and the labeled PE acceptors in the bilayer. Figure 6A shows the fluorescence spectrum of Pgp labeled with MIANS, and the absorption spectrum of NBD-PE, and Figure 6B shows the fluorescence spectrum of NBD-Pgp and the absorption spectrum of LRhoB-PE. Clearly, there is a large amount of spectral overlap (see Table 2 for values of the spectral overlap integral, J) and the value of R_o was close to 32 Å in each case, indicating that these two donor−acceptor pairs are highly suitable for FRET studies.

Since two donors are located within the same Pgp molecule, it is important to consider the possibility of energy transfer between them. The spectral overlap integrals (J) for NBD-NBD and MIANS-MIANS self-transfer were determined, and R_o values of 18.5 and 18.7 Å, respectively, were calculated (Table 2). Since the efficiency of energy transfer decreases dramatically with increasing distance (E depends on $1/R^6$; see eq 2), the efficiency of energy transfer between two residues with R_o of 18.5 Å located 30 Å apart is very small ($E = \sim 5\%$), compared to two residues with R_o of 32 Å ($E = \sim 60\%$). Thus, energy transfer between two NBD groups and two MIANS groups within a single Pgp molecule is relatively unimportant compared to energy transfer from labeled Pgp donors to lipid acceptors.

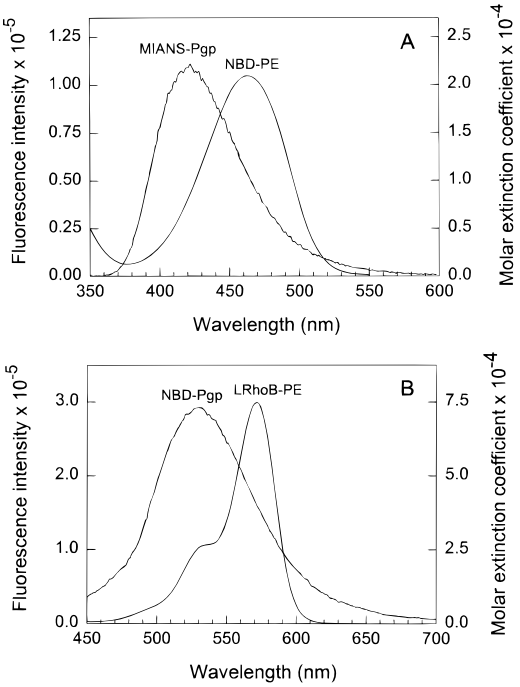

FIGURE 6: Overlap of the fluorescence emission spectra of the donors with the UV−visible absorption spectra of the acceptors used in this study. (A) Fluorescence emission spectrum of MIANS-Pgp (λ_{ex} = 322 nm, left scale) and the UV−visible absorption spectrum of NBD-PE (right scale). (B) Fluorescence emission spectrum of NBD-Pgp (λ_{ex} = 465 nm, left scale) and the UV−visible absorption spectrum of LRhoB-PE (right scale).

Table 2: Spectral Parameters for Donor and Acceptor Pairs[a]

FRET donor	FRET acceptor	quantum yield, Q_D	overlap integral, J ($cm^3\ M^{-1}$)	R_o (Å)
NBD-Pgp	LRhoB−PE	0.023	2.595×10^{-13}	31.93
MIANS-Pgp	NBD-PE	0.148	4.384×10^{-14}	32.38
NBD-Pgp	NBD-Pgp	0.023	9.876×10^{-15}	18.52
MIANS-Pgp	MIANS-Pgp	0.148	1.639×10^{-15}	18.72

[a] The refractive index, n, was taken as 1.33, and the orientation factor, κ^2, was assumed to be 2/3 (see Materials and Methods).

When designing an experimental system to measure energy transfer, the protein must be isolated in the bilayer, so that there are no other protein donors within the range in which FRET can occur. For R_o values in the range 40−60 Å, significant energy transfer will occur from a central protein donor to a lipid acceptor in the first 8−10 shells of lipid; energy transfer becomes negligible beyond this distance (*13*). It was calculated that the effect of neighboring protein molecules is small when lipid:protein mole ratios exceed 200:1 (*13*). We have more than adequately satisfied this criterion in the present study by reconstituting Pgp at a lipid:protein mole ratio of 1420:1. In addition, given the small values of R_o for donor−donor energy transfer, FRET between Pgp molecules adjacent in the bilayer would be expected to be negligible at this lipid:protein ratio if the protein is randomly distributed in the membrane. To rule out the possibility that Pgp molecules are associated with each other, NBD-Pgp and MIANS-Pgp were co-reconstituted into proteoliposomes at a lipid:protein mole ratio of 1420:1. No energy transfer was observed between MIANS and NBD, suggesting that Pgp does not aggregate in the bilayer under these conditions. Given that the thickness of the lipid bilayer

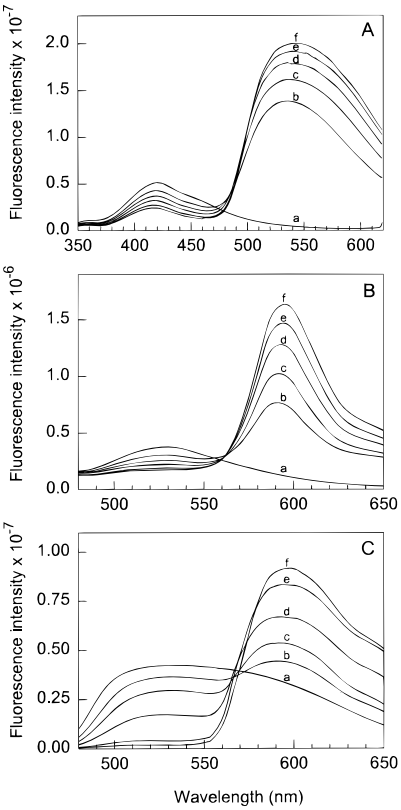

FIGURE 7: Fluorescence emission spectra demonstrating fluorescence energy transfer between donors and acceptors. Reconstituted proteoliposomes were made up of egg PC and egg PE containing increasing mole fractions of either NBD-PE or LRhoB-PE as indicated below (mole ratio of egg PC to total PE = 1:1). (A) Fluorescence emission spectra of MIANS-Pgp (λ_{ex} = 322 nm) in the presence of increasing mole fractions of the acceptor NBD-PE: 0 (a), 0.025 (b), 0.05 (c), 0.075 (d), 0.1 (e), and 0.15 (f). The total phospholipid:Pgp ratio was 1420:1 on a mole basis. (B) Fluorescence emission spectra of NBD-Pgp (λ_{ex} = 465 nm) in the presence of increasing mole fractions of the acceptor LRhoB-PE: 0 (a), 0.025 (b), 0.05 (c), 0.075 (d), 0.1 (e), and 0.15 (f). The total phospholipid:Pgp mole ratio was 1420:1. (C) Fluorescence emission spectra of NBD-PE in the presence of increasing mole fractions of the acceptor LRhoB-PE: 0 (a), 0.005 (b), 0.01 (c), 0.02 (d), 0.04 (e), and 0.06 (f). The mole ratio of total phospholipid to NBD-PE was 100:1. Emission bandwidths were 4 nm.

used in these experiments is around 50−55 Å, FRET from a donor on one side of the bilayer to an acceptor in the opposing leaflet will also be negligible.

When excited at 322 nm, the fluorescence of MIANS-Pgp progressively decreased when the protein was reconstituted in the presence of increasing mole fractions of the acceptor NBD-PE (Figure 7A). Concomitantly, sensitized emission of fluorescence at 540 nm by the NBD-PE acceptor was clearly evident. A similar decrease in NBD-Pgp fluorescence intensity was observed in the presence of increasing mole fractions of LRhoB-PE in the bilayer, accompanied by sensitized fluorescence from LRhoB-PE at 590 nm (Figure 7B). Energy transfer between NBD-PE and LRhoB-PE, where both fluorescent probes are located within the headgroup region of the bilayer, is shown in Figure 7C for comparison.

As indicated in Figure 8A, the relative intensity of NBD-Pgp fluorescence decreases with increasing mole fraction of LRhoB-PE in the bilayer. The quenching of NBD fluorescence by LRhoB-PE is more efficient when the NBD

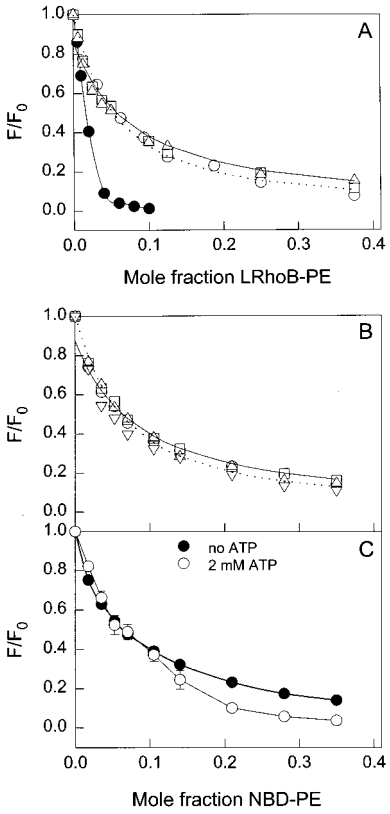

FIGURE 8: Curves fitting the FRET data from the various donor and acceptor systems to the models of Dewey and Hammes (solid lines) and Koppel et al. (dotted lines). (A) Fitting of the data for energy transfer from NBD-Pgp to LRhoB-PE (open symbols represent results from three independent experiments), and from NBD-PE to LRhoB-PE (●); (B) fitting of the data for energy transfer from MIANS-Pgp to NBD-PE in the absence of ATP (open symbols represent results from four independent experiments); (C) energy transfer from MIANS-Pgp to NBD-PE in the absence (●) and presence (○) of 2 mM ATP. Data points represent the mean of four independent experiments in each case; the data points in the absence of ATP are the mean of the four data sets shown in (B).

fluorophore is linked to the phospholipid headgroup of PE, rather than to the cysteine residues within the NB domains of the Pgp molecule (Figure 8A). This indicates that the catalytic sites of Pgp are located some distance away from the bilayer surface. For the MIANS-Pgp/NBD-PE donor−acceptor pair, the fluorescence of the donor is again progressively quenched by an increasing mole fraction of acceptor in the bilayer (Figure 8B).

The efficiency of FRET depends on the surface density of acceptors, and the distance between the protein-bound donor and the lipid headgroup acceptor. Analysis of FRET needs to take into account the distribution of fluorescence acceptors in the plane of the membrane. The approach of Koppel et al. (*30*) assumes that the lipid acceptors are randomly distributed on the surface of a sphere a distance *h* above or below the position of the donor on the protein. The second approach (*31*) assumes that the lipid acceptors are uniformly distributed on one plane, and the donors on the protein lie in another parallel plane, separated by a distance *h* from the parallel plane containing the donors. When the FRET quenching data were fitted to the equations of Koppel and co-workers, and of Dewey and Hammes, the values of *h* extracted were very similar in each case, 31−35 Å (see Table 3). In addition, as shown in Figure 8A,B, both data sets fitted well to the theoretical quench curves which are predicted by either method of analysis for these values of *h*. If a protein is labeled at two locations, and the two sites are not situated at very different distances from the membrane, then the value of *h* estimated by FRET will be an average of the two. On the other hand, if the two sites of labeling have large differences in their distance from the membrane, then the FRET data would not be expected to correspond to the theoretical quench curves. Since the data sets for both donor−acceptor pairs fit the theoretical predictions very well, this indicates that the two sites at which Pgp is labeled are positioned roughly equidistant from the bilayer, and the calculated value of *h* is an average over both sites. These results suggest that the two NB domains of Pgp are arranged approximately equivalently with respect to the membrane surface.

Table 3: Estimated Distances between the ATPase Catalytic Sites of Pgp and the Lipid Bilayer

FRET donor	FRET acceptor	conditions	estimated distance (Å): K method[a]	estimated distance (Å): D−H method[b]
NBD-Pgp	LRhoB−PE	no ATP	31.4 ± 0.5	33.1 ± 0.7
MIANS-Pgp	NBD-PE	no ATP	34.1 ± 0.7	34.8 ± 0.9
MIANS-Pgp	NBD-PE	2 mM ATP	does not fit	does not fit

[a] See ref *30*; data were fitted to eq 8, and the value of *h* was extracted. [b] See ref *31*; data were fitted to eqs 10−12, and the value of *h* was extracted.

When saturating concentrations of ATP were added to MIANS-Pgp in bilayers containing NBD-PE, and the quenching arising from FRET was determined again, the results were substantially different from those measured in the absence of ATP (Figure 8C). At low mole ratios of the acceptor NBD-PE (<0.05), there was less quenching of MIANS-Pgp due to energy transfer, whereas at mole ratios of acceptor >0.1, the quenching was substantially higher. The data set collected in the presence of ATP did not fit the equations of either Koppel and co-workers or Dewey and Hammes. These results suggest that the two NB domains of Pgp interact differently with the NBD-PE lipid acceptor following ATP binding.

DISCUSSION

There is currently a paucity of structural information for all members of the ABC superfamily. The recent development of fluorescence techniques for the study of the Pgp multidrug transporter has opened the door to the use of spectroscopy to measure distances on a molecular scale. In the present study, we use energy transfer to provide the first estimates of the distance between a defined site in the NB domains of Pgp and the membrane surface. The FRET donor consisted of highly purified fluorescently labeled Pgp, reconstituted into lipid bilayer vesicles containing a headgroup-labeled phospholipid as the acceptor.

Previous work in our laboratory reported the site-specific fluorescent labeling of Pgp on two cysteine residues, one within each NB domain (Cys 428 and 1071), using the sulfhydryl-specific agent MIANS. In the present work, we have extended this approach to label Pgp with the fluorescent probe NBD-Cl, which has been widely used as a covalent inhibitor of ATP-driven transporters. Senior and co-workers

reported that NBD-Cl treatment of MDR cell plasma membrane vesicles (*35*), or purified Pgp in proteoliposomes (*36*), resulted in loss of Pgp ATPase activity which was partially protected by the presence of ATP. Similar results were found in the present study. Al-Shawi and Senior (*35*) also indicated that only one molecule of NBD-Cl reacted with each molecule of Pgp, and they suggested that a lysine residue on Pgp was labeled, rather than a cysteine. In contrast, we have obtained experimental data which clearly indicate that under our labeling conditions, 2 mol of NBD is incorporated per mole of Pgp, and the two labeled residues are the same cysteine residues which react with MIANS. Analysis by both UV−visible and fluorescence spectroscopy indicated that it is the cysteine residues that are labeled. In addition, we found that the γ-NH_2 group of NAc-Lys-ME reacted with NBD-Cl at least 30-fold more slowly than the −SH group of NAc-Cys at pH 7.5, but reacted relatively faster at pH 9.5 (data not shown). Pgp reacted with NBD-Cl rapidly at pH 7.5, again suggesting that the −SH group is the target of labeling. Labeling of Pgp with MIANS blocked reaction with NBD-Cl, and vice versa, indicating that the same cysteine residues are labeled by both reagents. Thus, two probes, with different chemical structures and fluorescent characteristics, can be introduced into the same location within the catalytic site of the NB domains of Pgp. This feature allowed us to conduct two parallel sets of experiments to estimate the distance between the probe and the membrane surface, providing a valuable internal check on the validity of the results. Spectroscopic characterization of NBD-labeled Pgp indicated that the probe was located in a relatively hydrophobic environment, confirming previous results obtained with MIANS-labeled Pgp (*11*).

In the present study, purified Pgp labeled with MIANS or NBD was reconstituted into lipid bilayer vesicles, together with variable amounts of the labeled lipids NBD-PE or LRhoB-PE, which were incorporated into the bilayer. Fluorescence experiments showed that MIANS-Pgp/NBD-PE and NBD-Pgp/LRhoB-PE were highly suitable donor and acceptor pairs for distance measurements by FRET. Two different methods of analysis of the FRET data, using the two different donor−acceptor pairs, give very similar results, which provides confidence in their validity, and suggests that the various assumptions and approximations used in the theoretical models are satisfactory.

In all cases, the separation between the labeled cysteine residues on Pgp and the surface containing the lipid-bound fluor fell in the narrow range of 31−35 Å. Both the NBD group and the rhodamine group of labeled PE are located close to the glycerol backbone of the lipid, in the interfacial headgroup region of the bilayer which extends 15 Å below the bilayer surface (*13, 14, 37*). If we assume that the lipid-bound fluors are located a mean distance of 7.5 Å below the surface, this would place the labeled cysteine residues within the NB domains about 23.5−27.5 Å above the membrane.

Calculation of the expected volume of the NB domains, assuming that they are spherical, with a partial specific volume of 0.73 $mL \cdot g^{-1}$ and molecular mass of 29.5 kDa (*38*), leads to a diameter of ∼4 nm. Based on a low-resolution structure (to 2.5 nm) determined by electron microscopy with image enhancement (*10*), the Pgp molecule was seen as a cylinder 10 nm wide in the plane of the membrane and 8 nm deep, with two 3 nm lobes close to the membrane on the cytosolic side which were thought to be the NB domains. Therefore, both calculations and experimental evidence suggest that the NB domains of Pgp are 30−40 Å in diameter. The relative location of the labeled cysteine within the NB domain is not known. However, it seems likely that it would not be buried deep in the interior of the domain, since it is accessible to nucleotides and several aqueous quenching agents (*12*). If the active site is positioned centrally within the NB domain, or offset from the domain center toward the cytosol, and is 23.5−27.5 Å from the bilayer surface, this suggests that the NB domains are very close to, or perhaps in contact with, the membrane.

The ATPase activity of Pgp has an absolute requirement for membrane lipids (*39*), and different lipid species and lipid mixtures are able to modulate both the catalytic activity (*33*) and the stimulation of this activity by drugs and chemosensitizers (*40*). We have also determined that several kinetic parameters characterizing the binding and hydrolysis of ATP by Pgp (K_d for ATP binding, K_M and E_{act} for ATP hydrolysis) are directly influenced by the phase state of the lipid bilayer (*34*; Romsicki and Sharom, unpublished data). Others have shown that the NB domains of Pgp prefer to associate with the membrane (*41*). Taken together, this information suggests that the NB domains may be in intimate contact with the membrane surface, either the headgroups of the lipids themselves or intracytoplasmic loops of the membrane-embedded portion of the transporter. Results of the present study provide further evidence to support this proposal.

The data available thus far suggest that the ATPase catalytic sites of the two NB domains of Pgp have virtually identical local environments. Both NBD- and MIANS-labeled Pgp displayed a single-component fluorescence spectrum (*11* and this work), and a single class of fluors was observed during collisional quenching studies of MIANS-labeled Pgp (*12*). Binding of fluorescent nucleotide derivatives to Pgp also gave no indication of different classes of binding sites (*12*). The environment immediately surrounding the labeled cysteine residues at the ATPase catalytic site is hydrophobic, but also contains a positive charge (*11, 12*). In the present work, the fact that both sets of Pgp-PE quenching data collected in the absence of ATP fitted very well to theoretical models for a single protein-bound fluor suggests that the two NB domains are also positioned roughly equidistant from the bilayer under these conditions. Senior and co-workers (*42*) have proposed that Pgp operates via an alternating sites type of mechanism, such that only one NB domain is catalytically active at any point in time.

Addition of saturating concentrations of ATP to MIANS-Pgp reconstituted with LRhoB-PE led to a significant change in the shape of the FRET quenching curve. Notably, the data no longer fitted either of the theoretical models; quenching by NBD-PE was decreased slightly at low mole fractions of lipid acceptor, but increased substantially at higher mole fractions (Figure 8C). These results suggest that Pgp interacts differently with fluorescent PE when it is in the ATP-bound form. Evidence for a conformational change arising from binding of ATP to the NB domains of Pgp has been obtained from studies of MIANS quenching by three different agents (acrylamide, I^-, Cs^+) in the absence and presence of nucleotide (*12*). Pgp also displayed differences in amide exchange rates in the presence of ATP, again

suggesting the existence of a change in tertiary structure following ATP binding (*9*).

The fact that the quenching plot in the presence of ATP no longer fits the models might arise from the existence of an equilibrium between two or more different Pgp conformations in the ATP-bound form, which is shifted in the presence of PE. PE has been shown to greatly activate the ATPase activity of Pgp in a concentration-dependent fashion (*33*, *34*, *39*). Increasing mole ratios of PE might result in a progressive switch in conformation of the ATP-bound form of Pgp, resulting in activation of the ATPase activity, and could be reflected in the anomalous behavior noted in Figure 8C. PE may be an allosteric effector of ATPase function or, alternatively, a specific interaction might take place between the headgroup of this lipid and the NB domains. Such a direct interaction would be promoted by the preferential location of PE in the inner leaflet of the plasma membrane in mammalian cells, and the proximity of the NB domains to the cytoplasmic surface of the membrane as shown in this study.

REFERENCES

1. Higgins, C. F. (1992) *Annu. Rev. Cell Biol. 8*, 265−269.
2. Doige, C. A., and Ames, G. F. (1993) *Annu. Rev. Microbiol. 47*, 291−319.
3. Leveille-Webster, C. R., and Arias, I. M. (1995) *J. Membr. Biol. 143*, 89−102.
4. Germann, U. A. (1996) *Eur. J. Cancer 32A*, 927−944.
5. Bosch, I., and Croop, J. (1996) *Biochim. Biophys. Acta 1288*, F37−F54.
6. Sharom (1997) *J. Membr. Biol. 160*, 161−175.
7. Kast, C., Canfield, V., Levenson, R., and Gros, P. (1996) *J. Biol. Chem. 271*, 9240−9248.
8. Loo, T. W., and Clarke, D. M. (1995) *J. Biol. Chem. 270*, 843−848.
9. Sonveaux, N., Shapiro, A. B., Goormaghtigh, E., Ling, V., and Ruysschaert, J. M. (1996) *J. Biol. Chem. 271*, 24617−24624.
10. Rosenberg, M. F., Callaghan, R., Ford, R. C., and Higgins, C. F. (1997) *J. Biol. Chem. 272*, 10685−10694.
11. Liu, R., and Sharom, F. J. (1996) *Biochemistry 35*, 11865−11873.
12. Liu, R., and Sharom, F. J. (1997) *Biochemistry 36*, 2836−2843.
13. Gutierrez-Merino, C., Munkonge, F., Mata, A. M., East, J. M., Levinson, B. L., Napier, R. M., and Lee, A. G. (1987) *Biochim. Biophys. Acta 897*, 207−216.
14. Munkonge, F., East, J. M., and Lee, A. G. (1989) *Biochim. Biophys. Acta 979*, 113−120.
15. Teruel, J. A., and Gómez-Fernández, J. C. (1987) *Biochem. Int. 14*, 409−416.
16. Gómez-Fernández, J. C., Corbalán-García, S., Villalaín, J., and Teruel, J. A. (1994) *Biochem. Soc. Trans. 22*, 826−829.
17. Carraway, K. L., III, Koland, J. G., and Carione, R. A. (1990) *Biochemistry 29*, 8741−8747.
18. Remmers, A. E., and Neubig, R. R. (1993) *Biochemistry 32*, 2409−2414.
19. Yegneswaran, S., Wood, G. M., Esmon, C. T., and Johnson, A. E. (1997) *J. Biol. Chem. 272*, 25013−25021.
20. Peterson, G. L. (1983) *Methods Enzymol. 91*, 95−119.
21. Romsicki, Y., and Sharom, F. J. (1997) *Biochemistry 36*, 9807−9815.
22. Doige, C. A., Yu, X., and Sharom, F. J. (1992) *Biochim. Biophys. Acta 1109*, 149−160.
23. Birkett, D. J., Price, N. C., Radda, G. K., and Salmon, A. G. (1970) *FEBS Lett. 6*, 436−348.
24. Parker, C. A. (1968) *Photoluminescence of Solutions*, Elsevier Publishing Co., Amsterdam.
25. Lakowicz, J. R. (1983) *Principles of Fluorescence Spectroscopy*, Chapter 2, Plenum Press, New York.
26. Dale, R. E., Eisinger, J., and Blumberg, W. E. (1979) *Biophys. J. 26*, 161−193.
27. Mata, A. M., Stefanova, H. I., Gore, M. G., Khan, Y. M., East, J. M., and Lee, A. G. (1993) *Biochim. Biophys. Acta 1147*, 6−12.
28. Wu, C. W., and Stryer, L. (1972) *Proc. Natl. Acad. Sci. U.S.A.* 69, 1104−1108.
29. Goldberg, M. C. (1989) *Luminescence applications in biological, chemical, environmental, and hydrological science*, pp98−107, American Chemical Society, Washington, DC.
30. Koppel, D. E., Fleming, P. J., and Stritmatter, P. (1979) *Biochemistry 18*, 5450−5457.
31. Dewey, T. G., and Hammes, G. G. (1980) *Biophys. J. 32*, 1023−1036.
32. Wolber, P. K., and Hudson, B. S. (1979) *Biophys. J. 28*, 197−210.
33. Sharom, F. J., Yu, X., Chu, J. W. K., and Doige, C. A. (1995) *Biochem. J. 308*, 381−390.
34. Sharom, F. J. (1997) *Biochem. Soc. Trans. 25*, 1088−1096.
35. Al-Shawi, M. K., and Senior, A. E. (1993) *J. Biol. Chem. 268*, 4197−4206.
36. Urbatsch, I. L., Al-Shawi, M. K., and Senior, A. E. (1994) *Biochemistry 33*, 7069−7076.
37. Mazeres, S., Schram, V., Tocanne, J. F., and Lopez, A (1996) *Biophys. J. 71*, 327−335.
38. Dayan, G., Baubichon-Cortay, H., Jault, J.-M., Cortay, J.-C., Deléage, G., and Di Pietro, A. (1996) *J. Biol. Chem. 271*, 11652−11658.
39. Doige, C. A., Yu, X., and Sharom, F. J. (1993) *Biochim. Biophys. Acta 1146*, 65−72.
40. Urbatsch, I. L., and Senior, A. E. (1995) *Arch. Biochem. Biophys. 316*, 135−140.
41. Sharma, S., and Rose, D. H. (1995) *J. Biol. Chem. 270*, 14085−14093.
42. Senior, A. E., Al-Shawi, M. K., and Urbatsch, I. L. (1995) *FEBS Lett. 377*, 285−289.

BI973031O